ISSN 0006-3509, Biophysics, 2020, Vol. 65, No. 4, pp. 533–540. © Pleiades Publishing, Inc., 2020.
Russian Text © The Author(s), 2020, published in Biofizika, 2020, Vol. 65, No. 4, pp. 629–637.

MOLECULAR BIOPHYSICS

The Prospects of Metal Oxide Nanoradiosensitizers: The Effect of the Elemental Composition of Particles and Characteristics of Radiation Sources on Enhancement of the Adsorbed Dose

V. N. Morozov[a, b, *], A. V. Belousov[a], V. I. Zverev[c], A. A. Shtil[a, d, e], M. A. Kolyvanova[a, b], and P. V. Krivoshapkin[d]

[a] *Burnazyan Federal Medical Biophysical Center, Federal Medical Biological Agency of the Russian Federation, Moscow, 123182 Russia*

[b] *Emanuel Institute of Biochemical Physics, Russian Academy of Sciences, Moscow, 119334 Russia*

[c] *Department of Physics, Moscow State University, Moscow, 119991 Russia*

[d] *ChemBio Cluster, ITMO University, St. Petersburg, 191002 Russia*

[e] *Blokhin National Medical Research Center of Oncology, Moscow, 115478 Russia*

**e-mail: morozov.v.n@mail.ru*

Received October 31, 2019; revised April 2, 2020; accepted April 7, 2020

Abstract—Nanoparticles with a high atomic number are of interest as radiosensitizers for radiation therapy of cancer. A variety of nanoparticles and radiation sources makes the challenge of selecting their optimal combinations to achieve maximum irradiation efficacy relevant. In this work, we calculated the values of the dose enhancement factors of elemental compositions of metal oxide nanoparticles (Al_2O_3, TiO_2, MnO_2, Fe_2O_3 and Fe_3O_4, NiO, GeO_2, ZrO_2, CeO_2, Gd_2O_3, Tm_2O_3, HfO_2, Ta_2O_5, and Bi_2O_3), as well as GeO_2 and HfO_2 doped with the rare-earth elements lanthanum or ytterbium in combination with monochromatic photons (1–500 keV) and X-ray radiation corresponding to the radiation of kilovoltage X-ray therapy machines. At a nanoparticle concentration of 10 mg/mL, the maximum values of the dose enhancement factors were from 1.03 to 2.55 for monochromatic radiation and from 1.01 to 2.33 for the studied X-ray spectra. Doping GeO_2 with 20% lanthanum or ytterbium led to an increase in the maximum value of dose enhancement factors by ~10%. Doping HfO_2 did not lead to significant changes in the value of dose-enhancement factors. Thus, all studied elemental compositions of nanoparticles, with the exception of Al_2O_3 (a dose enhancement factor ~1.02), are promising for application in kilovoltage X-ray radiotherapy. At the same time, the complex dependence of dose enhancement factors on the spectral composition of X-ray radiation requires detailed studies of the impact of irradiation conditions on the magnitude of the radiomodifying effect of nanoparticles.

Keywords: nanoparticles, radiation therapy, radiosensitizers, dose enhancement factor

DOI: 10.1134/S0006350920040107

Radiation therapy is used for radical and palliative treatment of a wide range of neoplasms, as well as non-neoplastic diseases [1, 2]. Despite its intensive development, there is still a significant potential for increasing the efficacy of radiation therapy [3, 4]: the radioresistance of tumors and the dosage on the surrounding normal tissues can significantly limit the use of radiation therapy. Various methods for modifying the cell radiosensitivity, such as hyperbaric oxygenation [5], hyperthermia [6, 7], the use of chemical radiomodifiers, sensitizers, and protectors [8–14], allow an increase in the efficacy of irradiation.

Recently, nanotechnology products have attracted attention in this regard [15–17]. One promising class of radiosensitizers are nanoparticles that contain elements with a high (relative to biological tissues) atomic number (Z) [18–23]. The kilovoltage range of X-ray photon energies (30–300 keV) is considered the most promising for their use. Due to the high cross section of their interaction with radiation, nanoparticles demonstrated the highest efficacy in this region [24–26]; the technique of their use is called NEXT (Nanoparticles Enhanced X-ray Therapy) [27].

Nanotechnology offers a wide variety of nanoparticles for radiation therapy. Despite the fact that since the pioneering work in [28] the greatest attention has been paid to gold nanoparticles, other materials,

Abbreviations: DEF, dose enhancement factor.

including metal oxides, also attract interest [18, 23, 29, 30]. Due to their physicochemical properties, biocompatibility, wide possibilities of synthesis and modification of the crystal lattice, metal oxide nanoparticles are promising for a wide range of biomedical applications [31, 32]. Nanoparticles of oxides of titanium [33], iron [34, 35], thulium [36], cerium [37], hafnium [38, 39], tantalum [40], and bismuth [41] have demonstrated their efficiency as antitumor radiosensitizers.

To achieve the greatest effect of nanoparticles radiosensitization, it is necessary to optimize the combination of their parameters with irradiation conditions. Since the absorption of photon energy depends primarily on the elemental composition, the choice of material for nanoparticles, all other things being equal, will be determined by the properties of radiation. A wide range of photon sources with different spectral characteristics can be used in NEXT: X-ray therapy machines, sources for brachytherapy, and monochromatic radiation sources [42]. The published computer calculations of the nanoparticles radiosensitization efficacy were performed mainly for individual monoelement compositions of particles or a limited set of radiation sources [43–46]. Thus, the problem of selecting the optimal combinations of nanoparticles and irradiation conditions is still urgent. The question of the effect of doping nanoparticles also remains open. The purpose of this work was to calculate the absorbed dose enhancement for a number of elemental compositions of metal oxide nanoparticles, including those doped with rare-earth elements, when using radiation of different spectral compositions, namely, monochromatic photons and kilovoltage X-rays

.

MATERIALS AND METHODS

To assess the efficacy of the studied elemental compositions of nanoparticles, the dose enhancement factor (DEF) values were calculated. The DEF is defined as the ratio of the absorbed dose in the volume of interest in the presence of nanoparticles (D_2) to the absorbed dose in the same volume in their absence (D_1):

$$\mathrm{DEF} = D_2/D_1. \quad (1)$$

If the absorbed dose D_1 in some substance "1" is known, then under the conditions of electronic equilibrium, the absorbed dose D_2 in another substance "2" at the same point of the radiation field is determined by the expression

$$D_2 = \frac{(\mu/\rho)_2}{(\mu/\rho)_1} D_1, \quad (2)$$

where $(\mu/\rho)_i$ is the mass energy-absorption coefficient for the ith substance. In the case of monochromatic radiation and volumes that are not very large, the conditions for electronic equilibrium are fulfilled quite well; the error in determining the absorbed dose by formula (2) does not exceed 10%. In the case of continuous spectrum radiation, the region of interest must be located at a depth not less than the run of the fastest electrons released in matter by photons. In this case, the effective X-ray spectrum in the area of interest will differ from the nominal one. Here, expression (2) will be written as

$$D_2 = \frac{\int_0^{E_{\max}} \varphi(E) E \left(\frac{\mu(E)}{\rho}\right)_2 dE}{\int_0^{E_{\max}} \varphi(E) E \left(\frac{\mu(E)}{\rho}\right)_1 dE} D_1 = \frac{\overline{\left(\frac{\mu}{\rho}\right)_2}}{\overline{\left(\frac{\mu}{\rho}\right)_1}} D_1 = \overline{\left(\frac{\mu}{\rho}\right)_1^2} D_1. \quad (3)$$

In expression (3), $\varphi(E)dE$ denotes the flux of photons, whose energy lies in the interval $(E, E + dE)$. Finally, for X-ray radiation we have

$$\mathrm{DEF} = \overline{\left(\frac{\mu}{\rho}\right)_1^2}. \quad (4)$$

The values of the mass energy-absorption coefficient for various chemical elements were obtained in the XMuDat program [47] based on the data of [48]. For a substance that is a mixture of various chemical elements, the mass energy-absorption coefficients can be calculated as

$$\frac{\mu_{en}}{\rho} = \sum_i w_i \left(\frac{\mu_{en}}{\rho}\right)_i, \quad (5)$$

where $\left(\frac{\mu_{en}}{\rho}\right)_i$ is the mass energy-absorption coefficient for the ith element in the mixture and w_i is the mass content of this element in the mixture.

The absorbed dose enhancement was calculated for the following elemental compositions of metal oxide nanoparticles: Al_2O_3 ($Z_{Al} = 13$), TiO_2 ($Z_{Ti} = 22$), MnO_2 ($Z_{Mn} = 25$), Fe_2O_3 and Fe_3O_4 ($Z_{Fe} = 26$), NiO ($Z_{Ni} = 28$), GeO_2 ($Z_{Ge} = 32$, metalloid), ZrO_2 ($Z_{Zr} = 40$), CeO_2 ($Z_{Ce} = 58$), Gd_2O_3 ($Z_{Gd} = 64$), Tm_2O_3 ($Z_{Tm} = 69$), HfO_2 ($Z_{Hf} = 72$), Ta_2O_5 ($Z_{Ta} = 73$), and Bi_2O_3 ($Z_{Bi} = 83$). The concentration of nanoparticles in water was taken equal to 10 mg/mL. To assess the effect of doping on the DEF, the rare-earth elements La ($Z_{La} = 57$) and Yb ($Z_{Yb} = 70$) were selected. The content of the dopants in the elemental compositions of the nanoparticles was taken to be 20%.

The calculations were performed for monoenergetic photons with energies from 1 to 500 keV (with a step of 1 keV), as well as kilovoltage with spectral characteristics corresponding to the radiation of various X-ray therapy machines. The energy spectra for X-ray tubes with the parameters presented in Table 1 were calculated by the Monte Carlo method using a Geant4 toolkit [49]. A detailed description of

the method for calculating the X-ray spectra is given in [50].

RESULTS AND DISCUSSION

From a physical point of view, the mechanism of the radiomodifying action of nanoparticles with a high atomic number is based on local enhancement of the absorbed dose and the generation of secondary radiation. The radiosensitization efficacy of nanoparticles is determined by the increase in the absorbed energy of primary radiation and the productivity of its conversion into the energy of secondary particles. If the secondary radiation yield is affected by many parameters of nanoparticles [51–56], then the probability of interaction with primary photons is mainly determined by the value of the mass energy-absorption coefficient corresponding to a given elemental composition of nanoparticles.

Figure 1a shows the ratios of the mass energy-absorption coefficients for the studied elemental compositions and water. The dependences of the DEF of the studied elemental compositions of nanoparticles (10 mg/mL) on the photon energy for the case of monoenergetic radiation are shown in Fig. 1b. The energy at which the maximum DEF value for a given elemental composition of nanoparticles is observed corresponds to the optimal energy of monoenergetic radiation. When irradiated with photons of such energy, the greatest absorbed dose enhancement and, consequently, the greatest efficacy of radiosensitization, are expected. The following elemental compositions demonstrated the highest efficacy in various photon energy ranges: Bi_2O_3 (20–57 keV), CeO_2 (58–60 keV), Gd_2O_3 (61–70 keV), Tm_2O_3 (71–85 keV), HfO_2 (86–105 keV), and Bi_2O_3 (106–500 keV). Bi_2O_3 showed the highest DEF = 2.55. The maximum values of the DEF of CeO_2 (2.25), Gd_2O_3 (2.19), and Tm_2O_3 (2.11) turned out to be higher than those corresponding to elemental compositions with higher Z: HfO_2 (2.03) and Ta_2O_5 (2.04). The maximum DEF values of the elemental compositions TiO_2, MnO_2, Fe_2O_3, Fe_3O_4, NiO, and GeO_2 ranged from 1.17 to 1.51. A significant increase in the absorbed dose in the presence of Al_2O_3 was not found.

Table 1. The characteristics of the X-ray tubes used in simulation of X-ray spectra

Voltage, kVp	Anode material	Filtration*
300	W	0.4 mm Cu
250	W	1.6 mm Cu + 4.0 mm Al
200	W	1.2 mm Cu + 4.0 mm Al
160	W	Without additional filtration
110	W	1.3 mm Cu + 5.5 mm Al
85	W	2.0 mm Al
40	W	0.8 mm Al

* For all filtration options, a beryllium window with a thickness of 4.0 mm was taken into account by default.

In kilovoltage X-ray therapy machines (classical devices for superficial radiation therapy) X-ray tubes that generate photon radiation in the energy range from 30 to 300 keV are a radiation source. The spectral composition of radiation, in addition to the tube voltage, is determined by the design features (the anode material and the filters used) [57]. The calculated energy spectra of X-ray tubes (their characteristics are presented in Table 1) are shown in Fig. 2.

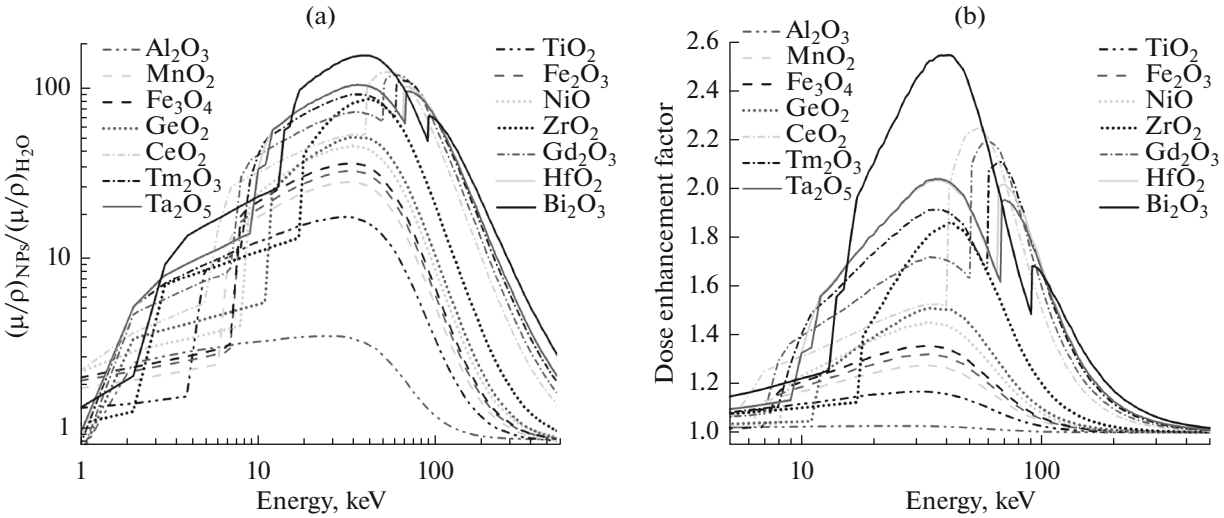

Fig. 1. (a) The ratio of the mass energy-absorption coefficients of the investigated elemental compositions of nanoparticles and water; (b) the dependences of the dose enhancement factor (DEF) of the elemental compositions of metal oxide nanoparticles (10 mg/mL) on the photon energy.

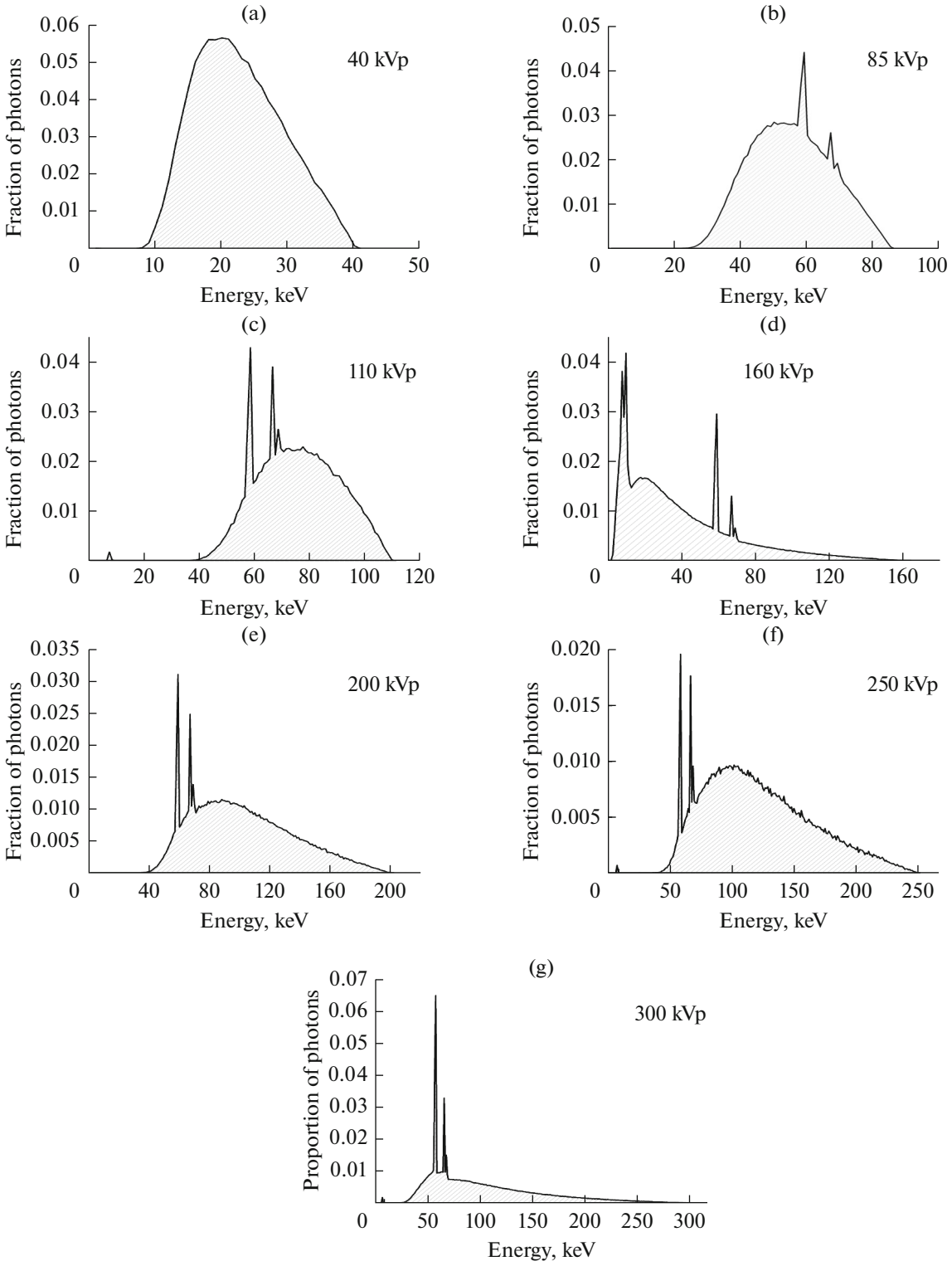

Fig. 2. The energy spectra of investigated X-ray tubes at voltages (kVp): (a) 40, (b) 85, (c) 110, (d) 160, (e) 200, (f) 250, and (g) 300.

The DEF values calculated for various combinations of nanoparticles and X-ray spectra are presented in Table 2. As in the case of monoenergetic radiation, Al_2O_3 showed the smallest increase in absorbed dose (≤2%). The absorbed dose enhancement by ~5–30% was found for TiO_2, MnO_2, Fe_2O_3, Fe_3O_4, NiO, and GeO_2. Significantly higher DEF values were demonstrated by ZrO_2, CeO_2, Gd_2O_3, Tm_2O_3, HfO_2, Ta_2O_5,

Table 2. The values of dose enhancement factor (DEF) for the studied elemental compositions of metal oxide nanoparticles for various X-ray spectra

Material	Maximum photon energy in the X-ray spectrum						
	40 keV	85 keV	110 keV	160 keV	200 keV	250 keV	300 keV
Al_2O_3	1.01	1.02	1.01	1.02	1.01	1.01	1.01
TiO_2	1.09	1.13	1.07	1.08	1.04	1.05	1.08
MnO_2	1.14	1.21	1.12	1.08	1.06	1.07	1.12
Fe_2O_3	1.16	1.25	1.14	1.08	1.09	1.08	1.14
Fe_3O_4	1.18	1.28	1.15	1.08	1.10	1.09	1.15
NiO	1.21	1.36	1.20	1.08	1.13	1.08	1.13
GeO_2	1.21	1.42	1.24	1.06	1.16	1.09	1.15
ZrO_2	1.21	1.73	1.46	1.10	1.30	1.18	1.29
CeO_2	1.25	1.99	1.93	1.18	1.64	1.43	1.54
Gd_2O_3	1.33	1.89	**1.96**	1.18	1.68	**1.47**	1.55
Tm_2O_3	1.41	1.89	1.90	1.17	1.67	1.44	1.45
HfO_2	1.45	1.93	1.86	1.17	1.66	1.44	1.46
Ta_2O_5	1.45	1.92	1.81	1.17	1.63	1.42	1.45
Bi_2O_3	**1.56**	**2.33**	1.88	**1.21**	**1.69**	**1.47**	**1.59**

The highest DEF values for a given X-ray spectrum are marked in bold.

and Bi_2O_3. However, all these values turned out to be significantly lower than the maximum DEF obtained for monoenergetic radiation.

The complex nature of the dependence of the DEF on the X-ray radiation spectral composition does not allow unambiguous conclusions about the selection of the optimal energy spectra for each elemental composition. At the same time, these data demonstrate that the highest DEF values do not always correspond to nanoparticles with higher Z [43]. Thus, for the spectra with maximum photon energies of 110 and 250 keV, it turned out that the DEF value for Bi_2O_3, which demonstrated the greatest increase in the absorbed dose among the entire investigated line of elemental compositions of nanoparticles, is lower than the DEF value for Gd_2O_3. Similarly, for spectra with maximum energies of 85, 110, and 300 keV, the higher DEF values corresponded to some elemental compositions with lower Z (for example, CeO_2 and Gd_2O_3). However, since the X-ray radiation spectra for machines from different manufacturers can differ significantly and the types of devices are not limited to those studied in this work, it is rather difficult to reveal the dependence of the efficacy of various elemental compositions of nanoparticles on the spectral characteristics of radiation sources. Moreover, as photons penetrate into a substance, the spectral composition of the radiation changes, which should also be taken into account in the calculations.

One distinctive feature of metal oxide nanoparticles is the wide possibilities of doping the crystal lattice, due to which they acquire new properties: luminescence in the ultraviolet, visible, and infrared ranges and the ability to act as contrast agents in magnetic resonance imaging [58–62]. At the same time, a change in the elemental composition of nanoparticles can affect the absorption of primary photons and the generation of secondary radiation, which, in turn, can affect the radiosensitization efficacy.

Figure 3 shows the dependences of the DEF on the photon energy for the GeO_2 (Fig. 3a) and HfO_2 (Fig. 3b) elemental compositions, both the original ones and those doped with the rare-earth elements La and Yb (20%). Such contents of dopants were chosen because they provide the luminescence effect with the preservation of the crystal structure of nanoparticles. Doping of GeO_2 led to an increase in the maximum DEF by ~12% (La) with a shift in the position of the maximum from 34 to 47 keV and by ~10% (Yb) without a significant shift. An increase in the DEF as a result of HfO_2 doping was not observed; on the contrary, the DEF of the elemental composition doped with 20% La turned out to be noticeably lower than the original in the energy range of 10–40 keV. A shift in the position of the DEF maximum for HfO_2 from 37 keV was observed when both dopants were used: up to 42 keV (La) and up to 69 keV (Yb).

The DEF values of the original and doped GeO_2 and HfO_2 for the spectra of X-ray therapy machines are given in Table 3. It can be seen that the DEF values of the doped GeO_2 compositions turned out to be significantly higher than the originals for the entire range

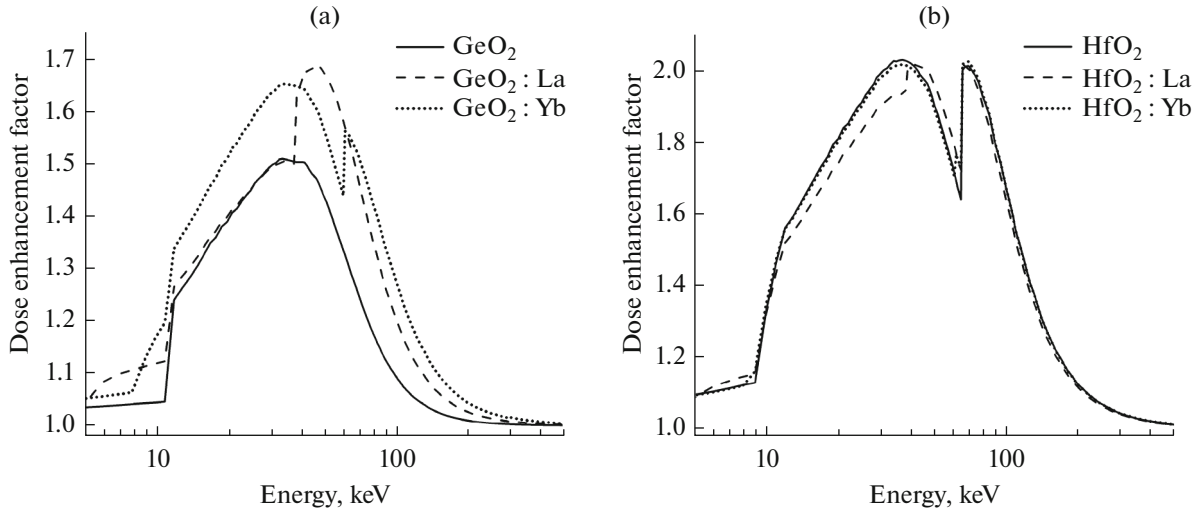

Fig. 3. The dependences of the dose enhancement factor (DEF) of original and 20% La- and 20% Yb-doped (a) GeO_2 and (b) HfO_2 elemental compositions on the photon energy.

of energy spectra. HfO_2 doping did not result in significant changes.

CONCLUSIONS

In this work, the efficacy of metal oxide nanoparticles as radiosensitizers for kilovoltage X-ray therapy was considered exclusively from a physical point of view. All the studied elemental compositions of nanoparticles, with the exception of Al_2O_3, demonstrated a significant increase in the absorbed dose (≥10%) in terms of clinical (and radiobiological) criteria, which indicates the prospects of their use in the NEXT. It should be noted that radiosensitization can be caused not only by physical factors, but also by the chemical and/or biological action of nanoparticles. Thus, the effect observed in the experiment can significantly exceed the theoretically predicted one.

The highest DEF values of the investigated elemental compositions of nanoparticles were obtained in combination with monoenergetic radiation; thus, its use can most effectively unleash their radiomodifying potential. It was found that differences in the spectral composition of X-ray can lead to a significant scatter in the DEF values of individual elemental compositions, which indicates the importance of further studies using a larger set of radiation sources. The results we obtained make it possible, to positively evaluate the effect of doping, since, in addition to acquiring new properties, the presence of dopants can increase the radiomodifying potential of nanoparticles, especially elemental compositions with low Z values.

Table 3. The values of dose enhancement factor (DEF) for original and 20% La- and 20% Yb-doped GeO_2 and HfO_2 elemental compositions for various X-ray spectra

Material	Maximum photon energy in the X-ray spectrum						
	40 keV	85 keV	110 keV	160 keV	200 keV	250 keV	300 keV
GeO_2							
GeO_2	1.21	1.42	1.243	1.060	1.156	1.092	1.152
GeO_2 : La	1.22	**1.59**	1.439	1.094	1.293	1.186	**1.265**
GeO_2 : Yb	**1.28**	1.57	**1.452**	**1.099**	**1.321**	**1.206**	1.251
HfO_2							
HfO_2	**1.45**	1.93	**1.86**	1.17	**1.66**	**1.44**	1.46
HfO_2 : La	1.41	**1.94**	**1.86**	1.17	1.65	1.43	**1.47**
HfO_2 : Yb	**1.45**	1.92	**1.86**	**1.18**	**1.66**	**1.44**	1.46

The highest DEF values for a given X-ray spectrum are marked in bold.

FUNDING

This work was financially supported by the Program for the Nuclear Medicine Development of the JSC Science and Innovations of the State Corporation ROSATOM (project AAAA-A19-119122590084-4) and the Russian Foundation for Basic Research (grant no. 18-29-11078).

COMPLIANCE WITH ETHICAL STANDARDS

The authors declare that they have no conflict of interest. This article does not contain any studies involving animals or human participants performed by any of the authors.

REFERENCES

1. R. Baskar, K. A. Lee, R. Yeo, et al., Int. J. Med. Sci. **9** (3), 193 (2012).
2. L. Gunderson and J. Tepper, *Clinical Radiation Oncology* (Elsevier, Philadelphia, 2016).
3. M. Baumann, M. Krause, J. Overgaard, et al., Nat. Rev. Cancer **16** (4), 234 (2016).
4. H. H. W. Chen and M. T. Kuo, Oncotarget **8** (37), 62742 (2017).
5. K. Stępień, R. P. Ostrowski, and E. Matyja, Med. Oncol. **33** (9), 101 (2016).
6. P. Kaur, M. D. Hurwitz, S. Krishnan, et al., Cancers (Basel) **3** (4), 3799 (2011).
7. J. C. Peeken, P. Vaupel, and S. E. Combs, Front. Oncol. **7**, 132 (2017).
8. C. K. Nair, D. K. Parida, and T. Nomura, J. Radiat. Res. **42** (1), 21 (2001).
9. P. Wardman, Clin. Oncol. (R. Coll. Radiol.) **19** (6), 397 (2007).
10. D. Citrin, A. P. Cotrim, F. Hyodo, et al., Oncologist **15** (4), 360 (2010).
11. R. M. Johnke, J. A. Sattler, and R. R. Allison, Future Oncol. **10** (15), 2345 (2014).
12. J. Linam and L. X. Yang, Anticancer Res. **35** (5), 2479 (2015).
13. M. Z. Kamran, A. Ranjan, N. Kaur, et al., Med. Res. Rev. **36** (3), 461 (2016).
14. H. Wang, X. Mu, H. He, et al., Trends Pharmacol. Sci. **39** (1), 24 (2018).
15. Y. Mi, Z. Shao, J. Vang, et al., Cancer Nanotechnol. **7** (1), 11 (2016).
16. L. A. Kunz-Schughart, A. Dubrovska, C. Peitzsch, et al., Biomaterials **120**, 155 (2017).
17. S. Goel, D. Ni, and W. Cai, ACS Nano **11** (6), 5233 (2017).
18. Retif, S. Pinel, M. Toussaint, et al., Theranostics **5** (9), 1030 (2015).
19. A. Subiel, R. Ashmore, and G. Schettino, Theranostics **6** (10), 1651 (2016).
20. S. Her, D. A. Jaffray, and C. Allen, Adv. Drug Deliv. Rev. **109**, 84 (2017).
21. S. Rosa, C. Connolly, G. Schettino, et al., Cancer Nanotechnol. **8** (1), 2 (2017).
22. L. Cui, S. Her, G. R. Borst, et al., Radiother. Oncol. **124** (3), 344 (2017).
23. Y. Liu, P. Zhang, F. Li, et al., Theranostics **8** (7), 1824 (2018).
24. W. N. Rahman, N. Bishara, T. Ackerly, et al., Nanomedicine **5** (2), 136 (2009).
25. D. B. Chithrani, S. Jelveh, F. Jalali, et al., Radiat. Res. **173** (6), 719 (2010).
26. S. Jain, J. A. Coulter, A. R. Hounsell, et al., Int. J. Radiat. Oncol. Biol. Phys. **79** (2), 531 (2011).
27. N. P. Praetorius and T. K. Mandal, Recent Pat. Drug Deliv. Formul. **1** (1), 37 (2007).
28. J. F. Hainfeld, D. N. Slatkin, and H. M. Smilowitz, Phys. Med. Biol. **49** (18), N309 (2004).
29. X. Y. Su, P. D. Liu, H. Wu, et al., Cancer Biol. Med. **11** (2), 86 (2014).
30. D. R. Cooper, D. Bekah, and J. L. Nadeau, Front. Chem. **2**, 86 (2014).
31. S. Andreescu, M. Ornatska, J. S. Erlichman, et al., in *Fine Particles in Medicine and Pharmacy*, Ed. by E. Matijević (Springer, Boston, 2012), pp. 57–100.
32. A. P. Ramos, M. A. E. Cruz, C. B. Tovani, et al., Biophys. Rev. **9** (2), 79 (2017).
33. C. Mirjolet, A. L. Papa, G. Crehange, et al., Radiother. Oncol. **108** (1), 136 (2013).
34. S. Khoei, S. R. Mahdavi, H. Fakhimikabir, et al., Int. J. Radiat. Biol. **90** (5), 351 (2014).
35. K. Khoshgard, P. Kiani, A. Haghparast, et al., Int. J. Radiat. Biol. **93** (8), 757 (2017).
36. E. Engels, M. Westlake, N. Li, et al., Biomed. Phys. Eng. Express **4** (4), 044001 (2018).
37. A. Montazeri, Z. Zal, A. Ghasemi, et al., Pharm. Nanotechnol. **6** (2), 111 (2018).
38. L. Maggiorella, G. Barouch, C. Devaux, et al., Future Oncol. **8** (9), 1167 (2012).
39. J. Marill, N. M. Anesary, P. Zhang, et al., Radiat. Oncol. **9**, 150 (2014).
40. R. Brown, S. Corde, S. Oktaria, et al., Biomed. Phys. Eng. Express **3** (1), 015018 (2017).
41. C. Stewart, K. Konstantinov, S. McKinnon, et al., Phys. Med. **32** (11), 1444 (2016).
42. E. Brauer-Krisch, J. F. Adam, E. Alagoz, et al., Phys. Med. **31** (6), 568 (2015).
43. J. C. Roeske, L. Nunez, M. Hoggarth, et al., Technol. Cancer Res. Treat. **6** (5), 395 (2007).
44. M. Hossain and M. Su, J. Phys. Chem. C Nanomater. Interfaces **116** (43), 23047 (2012).
45. S. J. McMahon, H. Paganetti, and K. M. Prise, Nanoscale **8** (1), 581 (2016).
46. V. N. Morozov, A. V. Belousov, G. A. Krusanov, et al., Optics Spectrosc. **125** (1), 104 (2018).
47. R. Nowotny, XMuDat: Photon Attenuation Data on PC (1998). https://www-nds.iaea.org/publications/iaea-nds/iaea-nds-0195.htm.
48. J. H. Hubbell and S. M. Seltzer, Tables of X-ray Mass Attenuation Coefficients and Mass Energy-Absorption Coefficients. http://www.nist.gov/pml/data/xraycoef (1996).
49. Geant4: A Simulation Toolkit. https://geant4.web.cern.ch.

50. A. V. Belousov, U. A. Bliznyuk, P. Y. Borschegovskaya, et al., Moscow. Univ. Phys. Bull. **69** (2), 157 (2014).
51. E. Lechtman, N. Chattopadhyay, Z. Cai, et al., Phys. Med. Biol. **56** (15), 4631 (2011).
52. B. Koger and C. Kirkby, Phys. Med. Biol. **62** (21), 8455 (2017).
53. N. Ma, F. G. Wu, X. Zhang, et al., ACS Appl. Mater. Interfaces **9** (15), 13037 (2017).
54. A. V. Belousov, V. N. Morozov, G. A. Krusanov, et al., Dokl. Phys. **63** (3), 96 (2018).
55. A. V. Belousov, V. N. Morozov, G. A. Krusanov, et al., Biomed. Phys. Eng. Express **4** (4), 045023 (2018).
56. A. V. Belousov, V. N. Morozov, G. A. Krusanov, et al., Biophysics **64** (1), 23 (2019).
57. F. M. Khan and G. P. Gibbons, *The Physics of Radiation Therapy* (Wolters Kluwer, Philadelphia, 2014).
58. A. Lauria, I. Villa, M. Fasoli, et al., ACS Nano **7** (8), 7041 (2013).
59. A. D. Furasova, A. F. Fakhardo, V. A. Milichko, et al., Colloids Surf. B. Biointerfaces **1**, 154 (2017).
60. G. Singh, B. H. McDonagh, S. Hak, et al., J. Mater. Chem. B **5**, 418 (2017).
61. I. Villa, C. Villa, A. Monguzzi, et al., Nanoscale **10** (17), 7933 (2018).
62. H. Deng, F. Chen, C. Yang, et al., Nanotechnology **29** (41), 415601 (2018).

Translated by G. Levit